

Probing the Z' sector of the minimal $B - L$ model at future Linear Colliders in the $e^+e^- \rightarrow \mu^+\mu^-$ process

L. Basso, A. Belyaev, S. Moretti and G.M. Pruna

*School of Physics and Astronomy, University of Southampton,
Highfield, Southampton SO17 1BJ, UK.*

Abstract

We study the capabilities of future electron-positron Linear Colliders, with centre-of-mass energy at the TeV scale, in accessing the parameter space of a Z' boson within the minimal $B - L$ model. In such a model, wherein the Standard Model gauge group is augmented by a broken $U(1)_{B-L}$ symmetry – with $B(L)$ being the baryon(lepton) number – the emerging Z' mass is expected to be in the above energy range. It turns out that such machines, as compared to the Large Hadron Collider, display an additional potential in discovering a Z' boson as well as in allowing one to uniquely study its properties at a level of precision well beyond that of the CERN machine.

1 Introduction

The $B - L$ (baryon number minus lepton number) symmetry plays an important role in various physics scenarios beyond the Standard Model (SM). Firstly, the gauged $U(1)_{B-L}$ symmetry group is contained in a Grand Unified Theory (GUT) described by a $SO(10)$ group [1]. Secondly, the scale of the $B - L$ symmetry breaking is related to the mass scale of the heavy right-handed Majorana neutrino mass terms providing the well-known see-saw mechanism [2] of light neutrino mass generation. Thirdly, the $B - L$ symmetry and the scale of its breaking are tightly connected to the baryogenesis mechanism through leptogenesis [3] via sphaleron interactions preserving $B - L$.

The minimal $B - L$ low-energy extension of the SM consists of a further $U(1)_{B-L}$ gauge group, three right-handed neutrinos and an additional Higgs boson generated through the $U(1)_{B-L}$ symmetry breaking. It is important to note that in this model the $B - L$ breaking can take place at the TeV scale, i.e., far below that of any GUT. This $B -$

L scenario therefore has interesting implications at the Large Hadron Collider (LHC), including new clean signatures from Z' , Higgs bosons and heavy neutrinos [4]–[5].

In the present paper we study the phenomenology related to the Z' sector of the minimal $B - L$ extension of the SM at the new generation of e^+e^- Linear Colliders (LCs) [6]. We consider the $e^+e^- \rightarrow \mu^+\mu^-$ channel as a representative process in order to study new signatures pertaining to the $B - L$ model. The LC environment is unique for Z' physics, for two main reasons. Firstly, if a Z' is found at the LHC, it could be the case that the underlying model is not easy (or even impossible) to identify at the hadronic machine. In contrast, the clean experimental environment of a LC is the ideal framework to establish the Z' line-shape (i.e. its mass and width) and to measure its couplings, thereby uniquely identifying the model and the observed spin-1 boson [7]. Secondly, we will also show that there exists further scope for a LC operating at TeV energies: specifically, to discover a Z' boson over regions of the $B - L$ parameter space which cannot be probed at all at the LHC, either directly through a resonance (when $\sqrt{s}_{e^+e^-} \geq M_{Z'}$) or indirectly through interference effects (when $\sqrt{s}_{e^+e^-} < M_{Z'}$). In both instances, a LC proves to be more powerful than the LHC in accessing the region of small Z' couplings.

This work is organised as follows. In the next section we describe the calculation techniques adopted. In Sect. 3 we present our numerical results. Finally, we conclude in Sect. 4.

2 Calculation

The study we present in this paper has been performed with the help of the CalcHEP package [8], in which the model under discussion had been previously implemented via the LanHEP tool [9], as already discussed in [4].

A feature specific to LCs is the presence of Initial State Radiation (ISR) and Beamstrahlung. For the former, CalcHEP [10] implements the Jadach, Skrzypek and Ward expressions of Ref. [11]. Regarding the latter, we adopted the parameterisation specified for the International Linear Collider (ILC) project in [7]:

$$\begin{aligned}
 \text{Horizontal beam size (nm)} &= 640, \\
 \text{Vertical beam size (nm)} &= 5.7, \\
 \text{Bunch length (mm)} &= 0.300, \\
 \text{Number of particles in the bunch (N)} &= 2 \times 10^{10}.
 \end{aligned}
 \tag{1}$$

There exists a certain subtlety in the comparison of the LHC and LC discovery potentials of a Z' boson. This comparison is not straightforward and ought to be performed carefully [12]–[13]. First of all, we need to compare consistent temporal collections of data. On the one hand, luminosities are different at the two kind of machines and so are

running schedules (a fixed energy at the LHC as opposed to the possibility of energy scans at the latter). In this connection, while comparing the scope of the two, we have assumed 100 fb^{-1} for the LHC throughout and $500(10) \text{ fb}^{-1}$ for LCs running at fixed energy (in energy scanning mode). On the other hand, data samples will be collected differently, chiefly, acceptance and selection procedures will be different. In this connection, we have assumed standard acceptance cuts (on muons) at the LHC and a typical LC¹,

$$\text{for the LHC : } \quad p_T^\mu > 10 \text{ GeV}, \quad |\eta^\mu| < 2.5, \quad (2)$$

$$\text{for a LC : } \quad E^\mu > 10 \text{ GeV}, \quad |\cos \theta^\mu| < 0.95. \quad (3)$$

Then, for both signal and background, we apply the following cut on the di-muon invariant mass, $M_{\mu\mu}$:

$$|M_{\mu\mu} - M_{Z'}| < \max \left(3\Gamma_{Z'}, 0.15\sqrt{\frac{M_{Z'}}{\text{GeV}}}\text{GeV} \right), \quad (4)$$

that is, a half window as large as either three times the width of the Z' -boson or the di-muon mass resolution², whichever the largest.

In our analysis we implement a suitable definition of signal significance, applicable to both the LHC and LC contexts, which we have done as follows. In the region where the number of both signal (s) and background (b) events is large enough (bigger than 20), we use a definition of significance based on Gaussian statistics, $\sigma \equiv s/\sqrt{b}$. Otherwise, in case of lower statistics, we exploited the Bityukov algorithm [16], which basically uses the Poisson ‘true’ distribution instead of the approximated Gaussian one. Hereafter, to ‘Observation’ it will correspond the condition $\sigma \geq 3$ and to ‘Discovery’ $\sigma \geq 5$.

Finally, as in [4], in the LHC case we used CTEQ6L [17], with $Q^2 = M_{Z'}^2$, as default Parton Distribution Functions (PDFs).

3 Results

Hereafter, to identify the Z' mass, width, couplings, etc. of our $B - L$ model we use the same notation as in [4]. Furthermore, we assume that the heavy neutrinos and Higgs states of the model have masses as in that paper³. This particular choice of the parameters

¹These cuts will then only be applied in the case of Figs. 1a and 1b (i.e., combination (2) and (4) for the LHC whereas (3) and (4) for a LC) and of Fig. 8 (again, combination (2) and (4) for the LHC) and not elsewhere.

²We assume the same di-muon mass resolution for both LHC and LC detectors, as, e.g., the CMS [14] and ILC [15] performances are very similar in this respect.

³For sake of completeness, we state here again the values we chose in [4]: $m_{\nu_h^1} = m_{\nu_h^2} = m_{\nu_h^3} = 200 \text{ GeV}$ and $m_{h_1} = 125 \text{ GeV}$, $m_{h_2} = 450 \text{ GeV}$, for the heavy neutrino and Higgs masses, respectively.

only affects the Z' width, in fact minimally (a few percents), so that our conclusions will be unaffected by it.

3.1 Experimental limits on Z' masses and couplings in $B - L$

Before proceeding to our signal-to-background analysis, we ought to define the parameter space of the $B - L$ model sector, compliant with current experimental constraints. Some stringent ‘indirect’ limits on the Z' mass-to-coupling ratio can be extracted from precision data (obtained at LEP and SLC), where the use of a four-fermion interaction already gives rather accurate results [18]. Despite this approach is well established, it is worth to note that more sophisticated techniques could change such bounds⁴. However, in the course of our analysis, we will be constraining ourselves to regions of masses and couplings that are immune from such constraints, as they lie well beyond the LEP and SLC limits (as well illustrated in some of our plots). Since the approximation used for the extraction of such limits is therefore irrelevant, we decided to quote and adopt here the more conservative result obtained by [19]:

$$\frac{M_{Z'}}{g'_1} \geq 7 \text{ TeV} \quad (5)$$

(which is not significantly lowered in the analysis of [18]: where $M_{Z'}/g'_1 \geq 6 \text{ TeV}$ is quoted). The most constraining ‘direct’ bounds come from Run 2 at Tevatron, chiefly from $q\bar{q} \rightarrow e^+e^-$ analyses. For definiteness, we take the CDF analysis of Ref. [20] using 2.5 fb^{-1} of data, which sets lower limits for Z' masses coming from several scenarios (e.g., a SM-like Z' and some E_6 string-inspired Z' models), but not for the $B - L$ case. Nonetheless, by rescaling the SM-like Z' coupling, we get for our $B - L$ setup, at 95% C.L.:

$$M_{Z'} \geq \begin{cases} 720 \text{ GeV} & \text{for } g'_1 = 0.1, \\ 1010 \text{ GeV} & \text{for } g'_1 = 0.5. \end{cases} \quad (6)$$

3.2 The LHC and LC potential in detecting Z' bosons in $B - L$

We start the presentation of our results by showing Fig. 1, which demonstrates the LHC and ILC discovery potential of a Z' boson over the $M_{Z'}-g'_1$ plane. Here, we define the signal as di-muon production via Z' exchange together with its interferences with the SM (i.e., γ and Z exchange) sub-processes whereas as background we take the SM di-muon production via γ and Z exchange. Both signal and background are then limited to the detector acceptance volumes and $M_{\mu\mu}$ invariant mass window described in the previous section. In Fig. 1a we considered a LC collecting data at the fixed energy of $\sqrt{s_{e^+e^-}} = 3 \text{ TeV}$. As one can clearly see, for $M_{Z'} > 800 \text{ GeV}$, the LC potential to explore the $M_{Z'}-g'_1$ parameter space goes beyond the LHC reach. For example, for $M_{Z'} = 1 \text{ TeV}$, the LHC

⁴For example, like those in Ref. [19], based on an effective Lagrangian parameterisation.

can discover a Z' if $g' \approx 0.007$ while a LC can achieve this for $g' \approx 0.005$. The difference is even more drastic for larger Z' masses as one can see from Tab. 1: a LC can discover a Z' with a 2 TeV mass for a g'_1 coupling which is a factor 8 smaller than the one for which the same mass Z' can be discovered at the LHC.

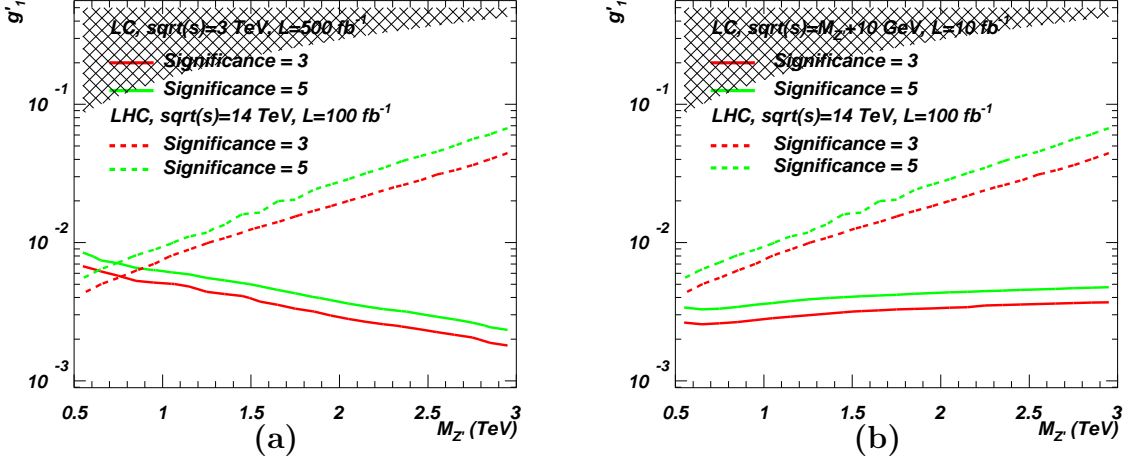


Figure 1: Significance contour levels plotted against g'_1 and $M_{Z'}$ both at the LHC for $L = 100 \text{ fb}^{-1}$ ($\sqrt{s_{pp}} = 14 \text{ TeV}$, dotted line) and: 1a LC for $L = 500 \text{ fb}^{-1}$, $\sqrt{s_{e^+e^-}} = 3 \text{ TeV}$, 1b LC for $L = 10 \text{ fb}^{-1}$, $\sqrt{s_{e^+e^-}} = M_{Z'} + 10 \text{ GeV}$, both in continuous line. The shaded areas correspond to the region of parameter space excluded experimentally, in accordance with eq. (5).

$M_{Z'} \text{ (TeV)}$	g'_1		
	LHC	LC ($\sqrt{s} = 3 \text{ TeV}$)	LC ($\sqrt{s} = M_{Z'} + 10 \text{ GeV}$)
1.0	0.0071	0.0050	0.0026
1.5	0.011	0.0040	0.0032
2.0	0.018	0.0028	0.0034
2.5	0.028	0.0022	0.0035

Table 1: Minimum g'_1 value accessible at the LHC and a LC for selected $M_{Z'}$ values in our $B-L$ model. At the LHC we assume $L = 100 \text{ fb}^{-1}$ whereas for a LC we take $L = 500 \text{ fb}^{-1}$ at fixed energy and $L = 10 \text{ fb}^{-1}$ in energy scanning mode.

In case of the energy scan approach, when the LC energy is set to $\sqrt{s_{e^+e^-}} = M_{Z'} + 10 \text{ GeV}$ (assuming 10 fb^{-1} of luminosity for each step), the parameter space can be probed even further for $M_{Z'} < 1.75 \text{ TeV}$, as shown in Fig. 1b. For example, for $M_{Z'} = 1 \text{ TeV}$, g'_1 couplings can be probed down to the 2.6×10^{-3} , following a Z' discovery. Furthermore, one can see that the parameter space corresponding to the mass interval $500 \text{ GeV} < M_{Z'} < 1 \text{ TeV}$, which the LHC covers better as compared to a LC with fixed energy, can be accessed

well beyond the LHC reach with a LC in energy scan regime. Altogether then, both an ILC, $\sqrt{s_{e^+e^-}} \leq 1$ TeV [21] and a Compact Linear Collider (CLIC, $\sqrt{s_{e^+e^-}} \leq 3$ TeV) [22] design may be able (over suitable regions of $B - L$ parameter space) to outperform the LHC.

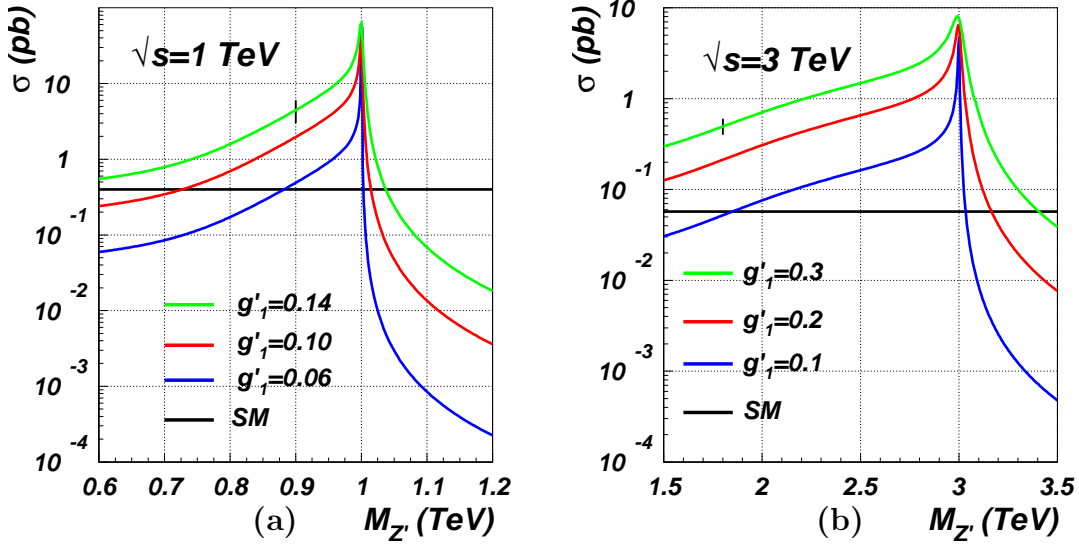


Figure 2: Cross section for the process $e^+e^- \rightarrow X \rightarrow \mu^+\mu^-$ for the signal ($X = Z'$) and the SM background ($X = \gamma, Z$, independent from $M_{Z'}$) plotted against $M_{Z'}$ at a LC for: 2a LC with $\sqrt{s_{e^+e^-}} = 1$ TeV, 2b LC with $\sqrt{s_{e^+e^-}} = 3$ TeV. (The black vertical bar refers to the mass and coupling combinations excluded by experimental data, to the left of it.)

Figs. 2a–2b present the general pattern of the Z' production cross section in comparison to the SM background as a function of $M_{Z'}$, for two fixed values of $\sqrt{s_{e^+e^-}}$, in such configurations that the Z' resonance can be either within or beyond the LC reach for on-shell production. The typical enhancement of the signal at the peak (now defined as the Z' sub-channel only) is two-three orders of magnitude above the background (again defined as γ, Z sub-channel only). This enhancement can onset (depending on the value of g'_1 , hence of $\Gamma_{Z'}$) several hundreds of GeV before the resonant mass and falls sharply as soon as the Z' mass exceeds the collider energy.

Similar effects can be appreciated in Figs. 3a–3b, where the Z' mass is now held fixed at two values and the LC energy is finely scanned around the resonance. In these last two plots, one can neatly appreciate the effects of the ISR, implying that the maximum cross section (i.e., the one at the Z' peak) is actually achieved for LC energy values higher than the Z' mass. Notice that this energy shift is proportional to the Z' width (i.e., the larger the stronger the g'_1 coupling) and is an example of the radiative return mechanism, whereby ISR effectively modulates $\sqrt{s_{e^+e^-}}$ over a wide mass range (below the maximum, the machine energy itself), so that, even at a fixed LC energy, one can reconstruct the $e^+e^- \rightarrow \mu^+\mu^-$ line shape by simply plotting the di-muon invariant mass distribution,

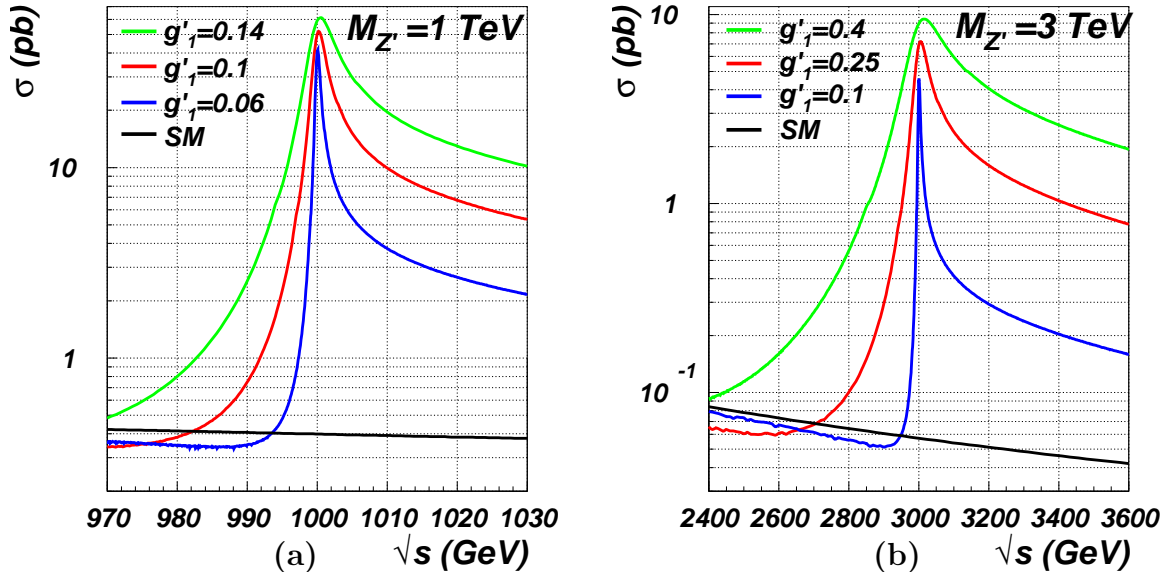


Figure 3: Cross section for the process $e^+e^- \rightarrow X \rightarrow \mu^+\mu^-$ cross section for the signal ($X = \gamma, Z, Z'$) and the SM background ($X = \gamma, Z$) plotted against $\sqrt{s_{e^+e^-}}$ (notice here the GeV scale) at a LC, for: 3a fixed $M_{Z'} = 1$ TeV, 3b fixed $M_{Z'} = 3$ TeV.

$M_{\mu\mu}$: see Fig. 4 (for an illustrative combination of $\sqrt{s_{e^+e^-}}$, $M_{Z'}$ and g'_1 's).

While the potential of future LCs in detecting Z' bosons of the $B-L$ model is well established whenever $\sqrt{s_{e^+e^-}} \geq M_{Z'}$, we would like to remark here upon the fact that, even when $\sqrt{s_{e^+e^-}} < M_{Z'}$, there is considerable scope to establish the presence of the additional gauge boson, through the interference effects that do arise between the Z' and SM sub-processes (Z and photon exchange). Even when the Z' resonance is beyond the kinematic reach of the LC, significant deviations are nonetheless visible in the di-muon line shape of the $B-L$ scenario considered, with respect to the the SM case. This is well illustrated in Figs. 5a–5b for the case of $\sqrt{s_{e^+e^-}}$ held fixed and $M_{Z'}$ variable (in terms of absolute rates) and in Figs. 6a–6b for the case of $M_{Z'}$ held fixed and $\sqrt{s_{e^+e^-}}$ variable (in terms of relative rates). Notice that in the studies presented in Figs. 5a–5b we have applied a useful kinematical, cut $M_{\mu\mu} > 200$ GeV, aimed at eliminating the production of a SM Z -boson due to the radiative return mechanism as well as enhancing the aforementioned interference effects. Incidentally, also notice that such strong interference effects do not onset in the case of the LHC, as it can clearly be seen from Fig. 7, owing to smearing due to the PDFs⁵.

In Figs. 5a–5b and Figs. 6a–6b we have assumed and indicated a 1% uncertainty band on the SM predictions (which is quite conservative). Under the assumption that SM di-muon production will be known with a 1% accuracy we would like to illustrate how

⁵See also Fig. 7 of Ref. [4].

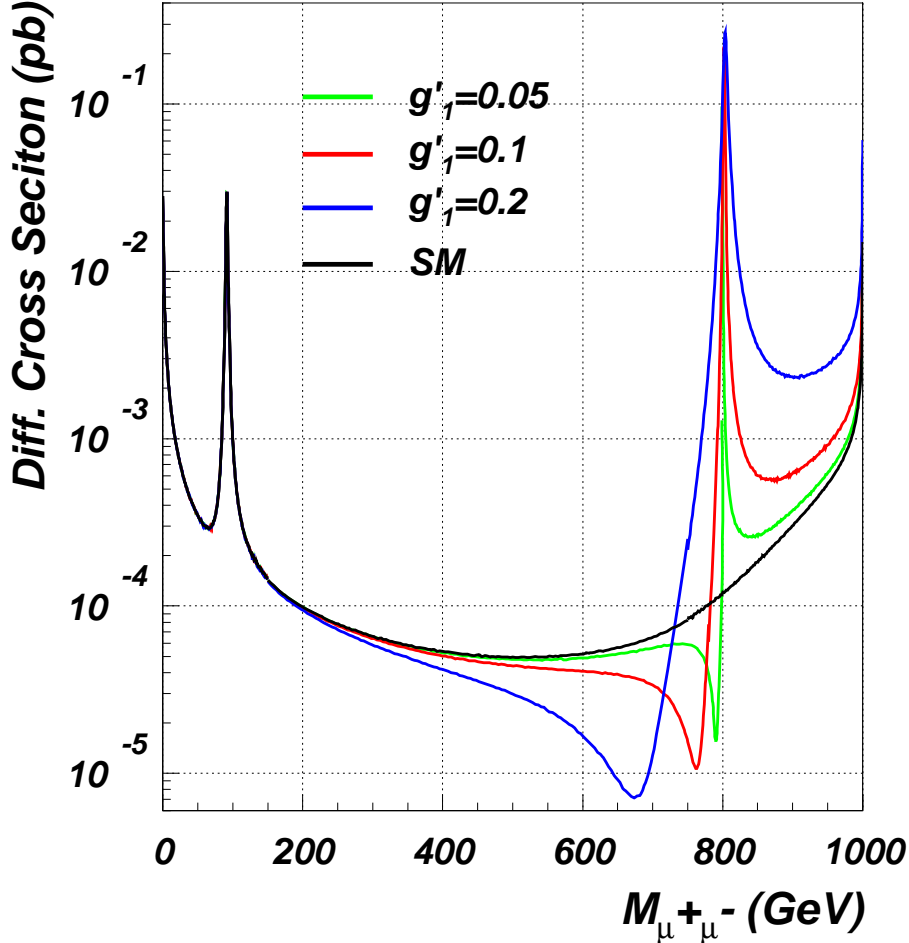


Figure 4: Cross section for process $e^+e^- \rightarrow \gamma, Z, Z' \rightarrow \mu^+\mu^-$ plotted against the di-muon invariant mass, $M_{\mu\mu}$, for $\sqrt{s_{e^+e^-}} = 1$ TeV, $M_{Z'} = 800$ GeV and $g'_1 = 0.05, 0.1$ and 0.2 .

the LHC 3σ observation potential of a heavy Z' (Fig. 8) is comparable to a LC indirect sensitivity to the presence of a Z' , even beyond the kinematic reach of the machine. This is shown in Tab. 2, which clearly shows that a CLIC type LC will be (indirectly) sensitive to much heavier Z' bosons than the LHC. For example, for $g'_1 = 0.1$, such a machine would be sensitive to a Z' with mass up to 10 TeV whilst the LHC can observe a Z' with mass below 4 TeV (for the same coupling). Even a LC with $\sqrt{s_{e^+e^-}} = 1$ TeV (a typical ILC energy) will be indirectly sensitive to larger $M_{Z'}$ values than the LHC, for large enough values of the g' coupling. For example, such a machine will be sensitive to a Z' with mass up to 7.5 TeV for $g'_1 = 0.2$ whilst the LHC would be able to observe a Z' only below 4.7 TeV or so (again, for the same coupling).

One interesting possibility opened up by such a strong dependence of the $e^+e^- \rightarrow \mu^+\mu^-$ process in the $B - L$ scenario on interferences (up to a 25% effect judging from, e.g.,

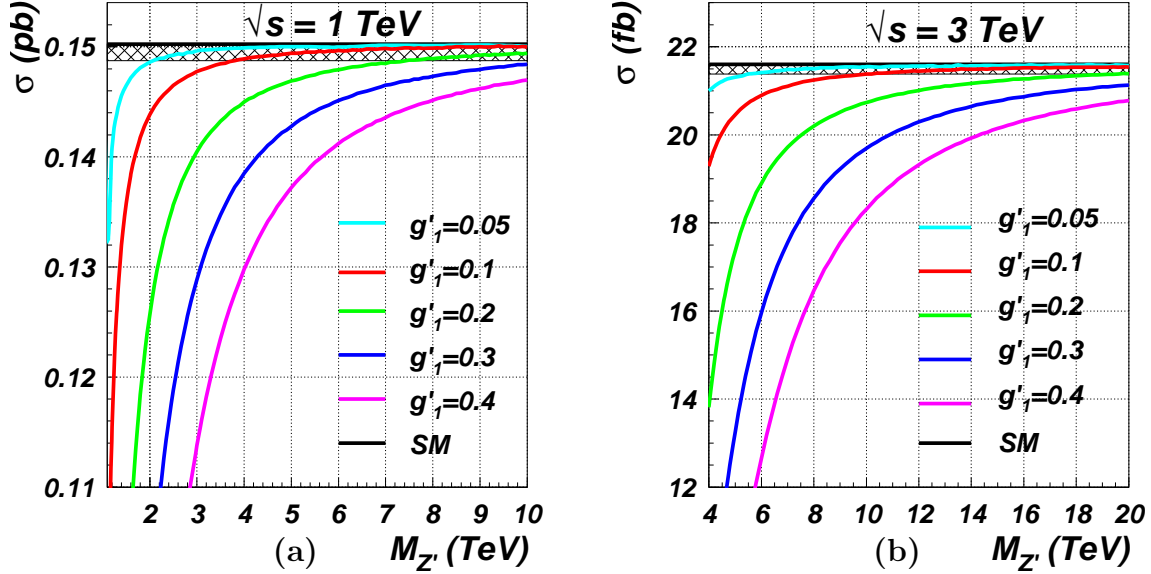


Figure 5: Cross section for the process $e^+e^- \rightarrow \gamma, Z, Z' \rightarrow \mu^+\mu^-$ plotted against $M_{Z'}$, for: 5a $\sqrt{s_{e^+e^-}} = 1$ TeV, 5b $\sqrt{s_{e^+e^-}} = 3$ TeV. Notice that we have implemented here the cut $M_{\mu\mu} > 200$ GeV. The shading corresponds to a 1% deviation from the SM hypothesis.

g'_1	$M_{Z'} \text{ (TeV)}$		
	LHC (3σ observation)	LC ($\sqrt{s} = 1$ TeV, 1% level)	LC ($\sqrt{s} = 3$ TeV, 1% level)
0.05	3.4	2.2	5.5
0.1	4.1	3.8	10
0.2	4.7	7.5	19.5

Table 2: Maximum $M_{Z'}$ value accessible at the LHC and a LC for selected g'_1 values in our $B - L$ model. At the LHC we assume $L = 100 \text{ fb}^{-1}$.

Fig. 6) is to see whether this potentially gives unique and direct access to measuring the g'_1 coupling. In fact, notice that in the case of Z' studies on or near the resonance (i.e., when $\sqrt{s_{e^+e^-}} \approx M_{Z'}$), the $B - L$ rates are strongly dependent on $\Gamma_{Z'}$ (hence on all couplings entering any possible Z' channel, that is, not only $\mu^+\mu^-$). Instead, when $\sqrt{s_{e^+e^-}} \ll M_{Z'}$ and $|\sqrt{s_{e^+e^-}} - M_{Z'}| \gg \Gamma_{Z'}$, one may expect that the role of the Z' width in such interference effects is minor, the latter being mainly driven by the strength of g'_1 . We prove this to be the case in Figs. 9a–9b, where we have artificially varied the Z' width by a factor of 10 (or even 50) in each set of $M_{Z'}$ and g'_1 values chosen. Here, it is clear that the dependence on $\Gamma_{Z'}$ is negligible (the more so the larger the difference $|\sqrt{s_{e^+e^-}} - M_{Z'}|$) whereas the one on either $M_{Z'}$ or g'_1 is always significant. Hence, in presence of a known value for $M_{Z'}$ (e.g., from a LHC analysis), one could extract g'_1 from a fit to the line shape. In fact, the same method, to access this coupling, could be exploited at future

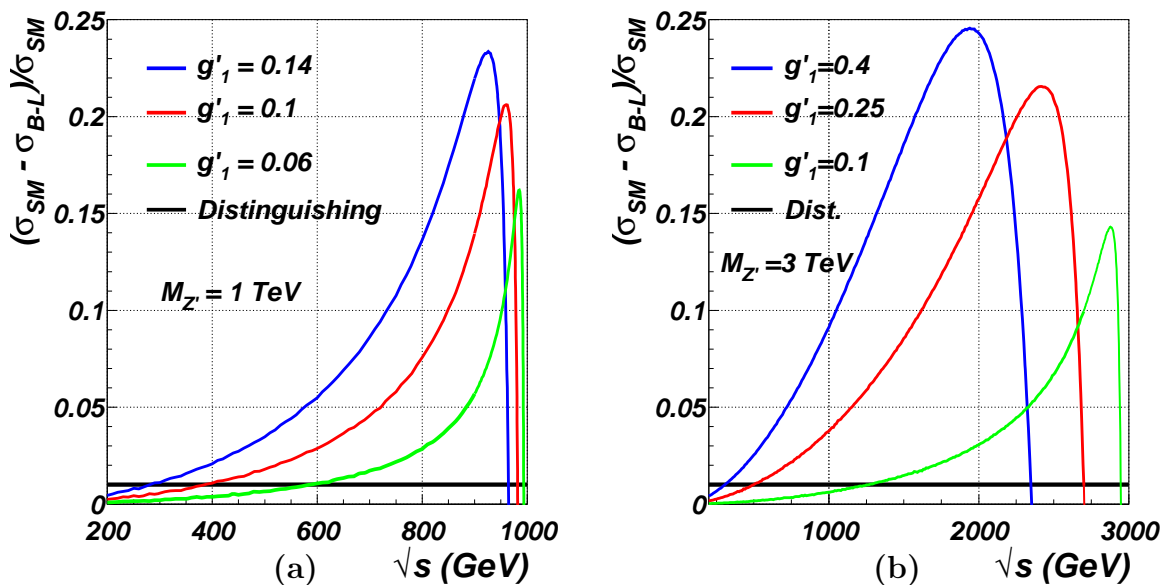


Figure 6: The relative difference for the cross section of the process $e^+e^- \rightarrow \mu^+\mu^-$ between the $B-L$ scenario and the SM plotted against $\sqrt{s_{e^+e^-}}$, for: 6a $M_{Z'} = 1$ TeV, 6b $M_{Z'} = 3$ TeV. The horizontal line corresponds to a 1% deviation from the SM hypothesis.

LCs independently of LHC inputs, as interference effects of the same size also appear when $\sqrt{s_{e^+e^-}} > M_{Z'}$: see again Fig. 4.

4 Conclusions

In summary, we have demonstrated the unique potential of future e^+e^- LCs in discovering Z' bosons produced resonantly via the $e^+e^- \rightarrow \mu^+\mu^-$ process within the minimal $U(1)_{B-L}$ extension of the SM. The scope in this respect of future LCs operating in the TeV range can be well beyond the reach of the LHC.

We have also presented the indirect sensitivity of LCs to a Z' below its production threshold, assuming a 1% combined uncertainty on the $e^+e^- \rightarrow \mu^+\mu^-$ production cross section. For example, for $\sqrt{s_{e^+e^-}} = 1(3)$ TeV, one can access Z' masses up to 2.2(5.5) TeV for $g'_1 = 0.05$. If the value of this coupling is four times larger, an ILC(CLIC) setup would be respectively sensitive to the range $M_{Z'} \leq 10(20)$ TeV.

Furthermore, in either kinematic configuration (i.e, for LCs with centre-of-mass energy below or above the Z' mass), it may be possible to access both the mass and (leptonic) couplings of the Z' , thereby constraining the underlying model, in parameter space regions fully compliant with experimental bounds.

These results have been obtained by exploiting parton level analyses based on the exact matrix element calculations appropriately accounting for the finite width and all

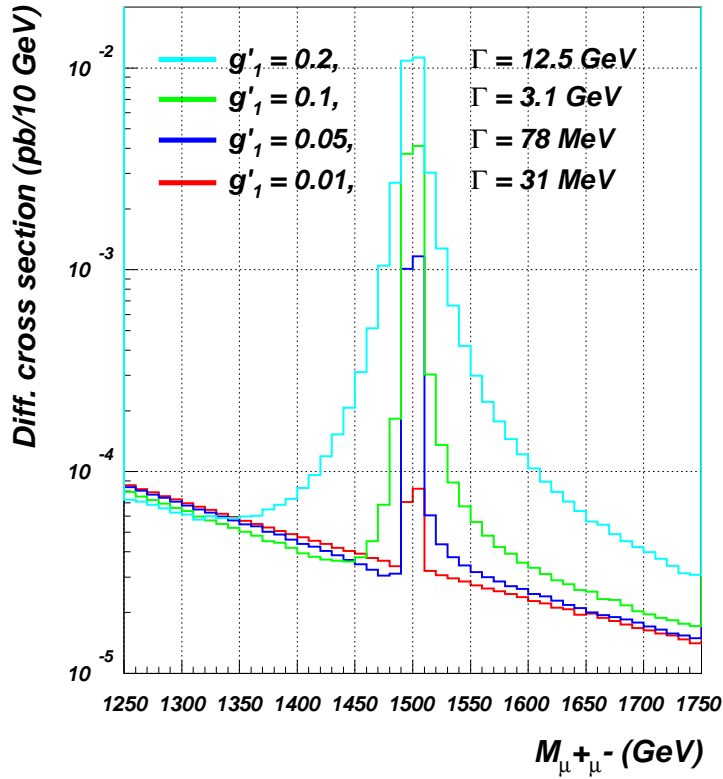


Figure 7: Differential cross section for the process $pp \rightarrow \mu^+\mu^-$ in the $B-L$ model plotted against $M_{\mu\mu}$ at the LHC ($\sqrt{s_{pp}} = 14$ TeV), with $M_{Z'}$ = 1.5 TeV, using a 10 GeV binning.

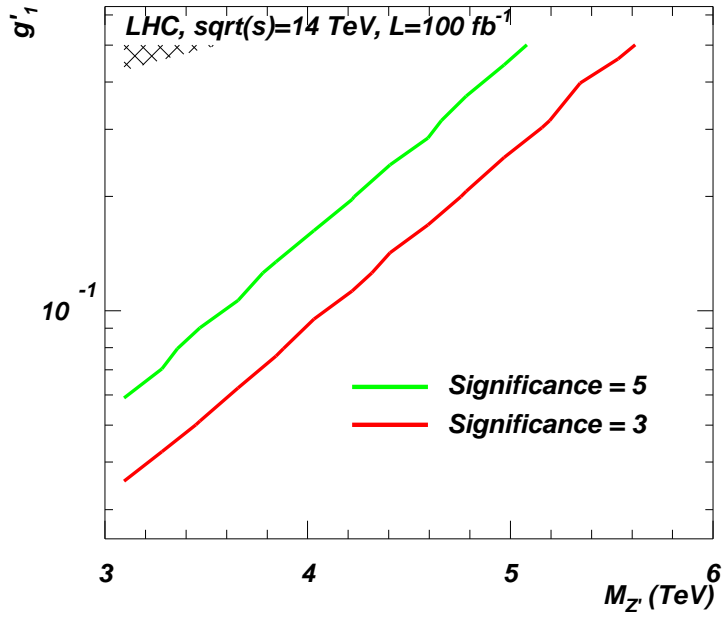


Figure 8: Significance contour levels plotted against g'_1 and $M_{Z'}$ at the LHC for $L = 100 \text{ fb}^{-1}$ ($\sqrt{s_{pp}} = 14 \text{ TeV}$, $M_{Z'} \geq 3 \text{ TeV}$). The shaded area corresponds to the region of parameter space excluded experimentally, in accordance with eq. (5).

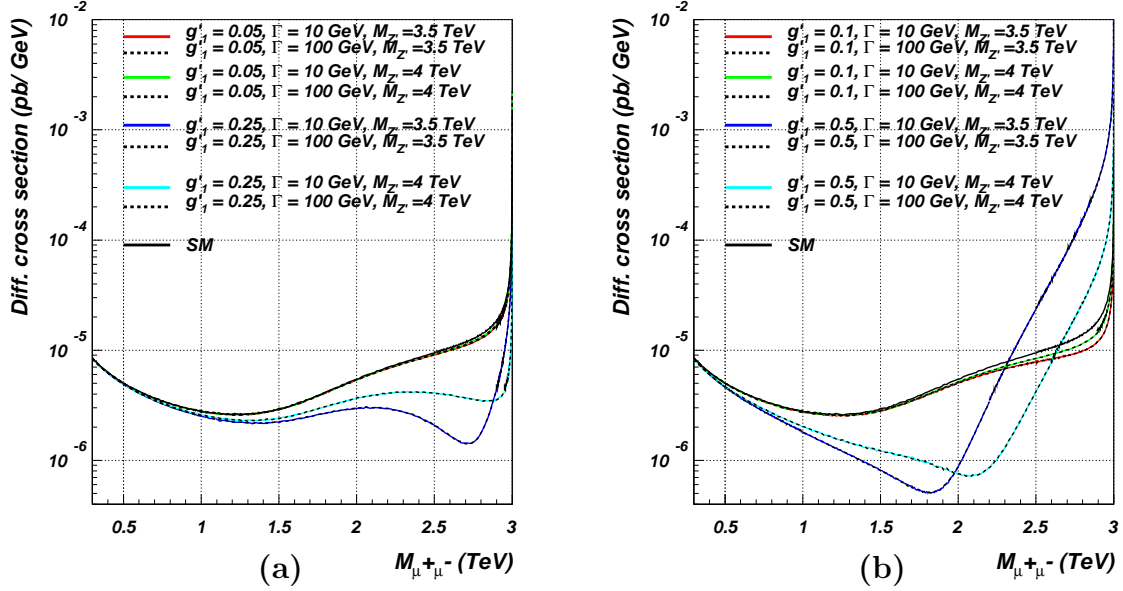


Figure 9: Differential cross section for the process $e^+e^- \rightarrow \mu^+\mu^-$ in the $B-L$ model plotted against $M_{\mu\mu}$, for several combinations of $M_{Z'}$ and g'_1 , treating $\Gamma_{Z'}$ as an independent parameter. Here, $\sqrt{s_{e^+e^-}} = 3$ TeV.

interference effects in the $e^+e^- \rightarrow \mu^+\mu^-$ channel. We have also taken into account beamstrahlung effects as well as general detector acceptance geometry. Finally, we would like to notice that there is further room to explore the LC potential to study Z' physics by exploiting beam polarisation and/or asymmetries in the cross section, which will be reported on separately [23].

Acknowledgements

LB and GMP thank Ian Tomalin for helpful discussions. AB thanks Andrei Nomerotsky and Tomáš Laštovička for useful discussions.

References

- [1] W. Buchmuller, C. Greub and P. Minkowski, Phys. Lett. B **267** (1991) 395.
- [2] P. Minkowski, Phys. Lett. B **67** (1977) 421; M. Gell-Mann, P. Ramond and R. Slansky, in *Supergravity*, eds. P. Van Nieuwenhuizen and D. Freedman (North-Holland, Amsterdam, 1979), p. 315; T. Yanagida, in *Proceedings of the Workshop on the Unified Theory and the Baryon Number in the Universe*, eds. O. Sawada and A. Sugamoto (KEK, Tsukuba, 1979), p. 95; S.L. Glashow, in *Quarks and Leptons*, eds.

- M.Lèvy *et al.* (Plenum, New York 1980), p. 707; R.N. Mohapatra and G. Senjanović, *Phys. Rev. Lett.* **44** (1980) 912.
- [3] M. Fukugita and T. Yanagida, *Phys. Lett. B* **174** (1986) 45.
- [4] L. Basso, A. Belyaev, S. Moretti and C. H. Shepherd-Themistocleous, arXiv:0812.4313 [hep-ph].
- [5] K. Huitu, S. Khalil, H. Okada and S.K. Rai, *Phys. Rev. Lett.* **101** (2008) 181802; W. Emam and S. Khalil, *Eur. Phys. J. C* **522** (2007) 625.
- [6] K. Abe *et al.*, [The ACFA Linear Collider Working Group], arXiv:hep-ph/0109166; T. Abe *et al.*, [The American Linear Collider Working Group], arXiv:hep-ex/0106055; arXiv:hep-ex/0106056; arXiv:hep-ex/0106057; arXiv:hep-ex/0106058; E. Accomando *et al.* [ECFA/DESY LC Physics Working Group], *Phys. Rept.* **299** (1998) 1; J.A. Aguilar-Saavedra *et al.*, [The ECFA/DESY LC Physics Working Group], arXiv:hep-ph/0106315; K. Ackermann *et al.*, preprint DESY-PROC-2004-01, DESY-04-123, DESY-04-123G.
- [7] J. Brau *et al.* [ILC Collaboration], arXiv:0712.1950 [physics.acc-ph].
- [8] A. Pukhov, arXiv:hep-ph/0412191.
- [9] A.V. Semenov, arXiv:hep-ph/9608488.
- [10] See: <http://www.ifh.de/~pukhov/calchep.html>.
- [11] S. Jadach and B. Ward, *Comp. Phys. Commun.* **56** (1990) 351; S. Jadach and M. Skrzypek, *Z. Phys. C* **49** (1991) 577.
- [12] J. A. Aguilar-Saavedra *et al.*, *Eur. Phys. J. C* **46** (2006) 43.
- [13] G. Weiglein *et al.* [LHC/LC Study Group], *Phys. Rept.* **426** (2006) 47.
- [14] G. L. Bayatian *et al.* [CMS Collaboration], preprint CERN-LHCC-2006-001, CMS-TDR-008-1.
- [15] T. Behnke *et al.* [ILC Collaboration], arXiv:0712.2356 [physics.ins-det].
- [16] S. I. Bityukov and N. V. Krasnikov, *Nucl. Instr. and Meth. A* **452** (2000) 518.
- [17] See: <http://durpdg.dur.ac.uk/hepdata/pdf.html>.
- [18] M. Carena, A. Daleo, B.A. Dobrescu and T.M.P. Tait, *Phys. Rev. D* **70** (2004) 093009.

- [19] G. Cacciapaglia, C. Csaki, G. Marandella and A. Strumia, Phys. Rev. D **74** (2006) 033011.
- [20] T. Aaltonen *et al.* [CDF Collaboration], Phys. Rev. Lett. **102** (2009) 031801.
- [21] A. Djouadi, J. Lykken, K. Monig, Y. Okada, M. J. Oreglia and S. Yamashita, arXiv:0709.1893 [hep-ph].
- [22] G. Guignard (editor) [The CLIC Study Team], preprint CERN-2000-008 (2000).
- [23] L. Basso, A. Belyaev, S. Moretti and G.M. Pruna, in preparation.